Kremen1 and Dickkopf1 control cell survival in a Wnt-independent manner.

Frédéric Causeret, Iffat Sumia, Alessandra Pierani

Kremen1 and Dickkopf1 control cell survival in a Wnt-independent manner

Running title: Kremen1 is a dependence receptor for Dickkopf1

Frédéric Causeret[1], Iffat Sumia and Alessandra Pierani[1]

Institut Jacques Monod, CNRS, UMR 7592, Univ Paris Diderot, Sorbonne Paris Cité F-75205 Paris, France

[1] Co-corresponding authors. Address: Institut Jacques Monod, Bâtiment Buffon 516B, 15 rue Hélène Brion, 75205 Paris Cedex 13, France. Phone : +33 157278128. Email: frederic.causeret@inserm.fr or alessandra.pierani@ijm.fr

Abstract

In multicellular organisms, a tight control of cell death is required to ensure normal development and tissue homeostasis. Improper function of apoptotic or survival pathways can not only affect developmental programs but also favor cancer progression. Here we describe a novel apoptotic signaling pathway involving the transmembrane receptor Kremen1 and its ligand, the Wnt-antagonist Dickkopf1. Using a whole embryo culture system, we first show that Dickkopf1 treatment promotes cell survival in a mouse model exhibiting increased apoptosis in the developing neural plate. Remarkably, this effect was not recapitulated by chemical Wnt-inhibition. We then show that Dickkopf1 receptor Kremen1 is a *bona fide* dependence receptor, triggering cell death unless bound to its ligand. We performed Wnt-activity assays to demonstrate that the pro-apoptotic and anti-Wnt functions mediated by Kremen1 are strictly independent. Furthermore, we combined phylogenetic and mutagenesis approaches to identify a specific motif in the cytoplasmic tail of Kremen1 which is (i) specifically conserved in the lineage of placental mammals and (ii) strictly required for apoptosis induction. Finally, we show that somatic mutations of *kremen1* found in human cancers can affect its pro-apoptotic activity, supporting a tumor suppressor function. Our findings thus reveal a new Wnt-independent function for Kremen1 and Dickkopf1 in the regulation of cell survival with potential implications in cancer therapies.

Keywords: Apoptosis | cell survival | dependence receptor | Dkk1 | Krm1

Abbreviations: CNS, central nervous system; COSMIC, catalogue of somatic mutations in cancer; DCC, deleted in colorectal cancer; Dkk, Dickkopf; ECD, extracellular domain; GFP, green fluorescent protein; HA, hemagglutinin; HEK, human embryonic kidney; ICD,

intracellular domain; Krm, Kringle-coding gene marking the eye and the nose; LRP, low-density lipoprotein receptor related protein; TCGA, the cancer genome atlas; TUNEL, terminal deoxynucleotidyl transferase dUTP nick end labeling; Wnt, wingless-related integration site

Introduction

In multicellular organisms, long-distance communication between cells is typically achieved by secreted ligands that diffuse through the extracellular medium and bind transmembrane receptors on target cells. Signal propagation through the plasma membrane is then achieved by receptor conformational changes upon ligand binding and classically involves modulation of enzymatic activity, interaction with intracellular partners or ion permeability. The classical view that transmembrane receptors only signal when bound to their ligand is now outdated, especially since the emergence of the dependence receptor concept. Dependence receptors do not form a family *per se*, but rather regroup a variety of receptors (transmembrane but also nuclear) that share the ability to trigger cell death unless bound to their respective ligand(s) [1]. Dependence receptors therefore display two signaling activities: a "positive" signaling in the presence of a ligand that can modulate various cellular processes (proliferation, differentiation, migration…), and a "negative" signaling in the absence of ligand consisting in the activation of a pro-apoptotic cascade downstream the receptor. To date, more than a dozen dependence receptors have been identified among which, DCC, Unc5A-D, Patched, TrkA/C, PlexinD1 and others [1-7], all of which play major roles during embryonic development, especially in the nervous system. Dependence receptors are also involved in cancer: since their apoptotic activity may allow to restrain cells within a ligand-rich environment and eliminate those that migrate away (such as metastatic cells), they were proposed to act as conditional tumor suppressors [1]. Accordingly, loss of function of a dependence receptor or overexpression of a ligand can confer a selective advantage to tumor cells.

Many signaling pathways involved during embryonic development are misregulated in cancers. Among them, the Wnt signaling pathway has been extensively studied in both developmental and cancer paradigms [8,9]. The Wnt1 ligand itself was first identified as a proto-oncogene [10] and later shown to be required for mammalian brain patterning [11]. Although Wnt

signaling was reported to elicit multiple cellular responses, most of the physiological effects described so far were shown to be mediated by the so-called canonical pathway: extracellular Wnt ligands bind transmembrane receptors of the Frizzled family associated to LDL receptor related protein (LRP) co-receptors, leading to the activation of an intracellular signaling cascade whose final effector, β-catenin, modulates the expression of target genes [12]. Critical regulations of the Wnt pathway occur at the extracellular level by means of secreted antagonists [13]. Dickkopf-1 (Dkk1) is one of such secreted inhibitors. It was shown to bind Kremen1/2 (Krm1/2) as well as LRP5/6 transmembrane receptors and subsequently inhibit Wnt downstream signaling [14-17]. During vertebrate embryonic development, Dkk1-mediated Wnt-antagonism in anterior regions is strictly required for head induction [18,19]. In cancers, Dkk1 function remains a matter of debate as it was proposed to act as either a positive or a negative factor depending on the context [20-22]. Such a discrepancy could reflect a yet unknown function for Dkk1 in addition to its well-characterized Wnt-inhibiting activity.

In this study, we unravel a new Wnt-independent anti-apoptotic function for Dkk1 and found it is mediated by its transmembrane receptor Krm1 which behaves as a dependence receptor.

Results

Dickkopf1 is a diffusible survival factor

Using a genetic cell ablation strategy in mice, we have previously identified a non cell-autonomous mechanism regulating cell survival during early (E8.5) embryonic mouse head development (Supplementary Figure 1a) [23]. We aimed at identifying the diffusible factor(s) and cognate receptor(s) that could be involved in such a process. We performed *in situ* hybridization for a range of secreted factors, as well as their transmembrane receptors, known to be involved in head development. Consistent with previous observations [19,24], we found that Dkk1 as well as its receptors Krm1/2 and Lrp6 are expressed in the anterior neural plate at E8.5 (Supplementary Figure 1b-f).

In order to test the possibility that Dkk1 regulates cell survival during forebrain development, we implemented a whole embryo culture strategy and assessed its ability to rescue apoptosis observed in our mouse model [23]. E7.5 embryos were dissected and maintained 24 h in culture prior to fixation and subsequent detection of apoptotic cells by TUNEL staining. Culture conditions allowed recapitulation of *in vivo* conditions, i.e. extensive apoptosis in the forebrain and midbrain of ablated embryos compared to wild-type littermates (Supplementary Figure 2). We found that treatment with soluble recombinant Dkk1 decreased in a dose-dependent manner the number of $TUNEL^+$ apoptotic cells observed in mutants (Figure 1), indicating that Dkk1 acts as a survival factor for embryonic mouse neural plate.

Dkk1 was shown to act as a potent inhibitor of Wnt signaling [18]. In order to determine whether it promotes survival in a Wnt-dependent manner, we applied endo-IWR1, a chemical inhibitor of Wnt canonical signaling [25], on ablated embryos. Unlike Dkk1 treatment, endo-IWR1 failed to recue apoptosis (Figure 1), indicating that Dkk1 anti-apoptotic function is Wnt-independent, and thus suggesting the possibility of a novel signaling pathway downstream Dkk1.

Dickkopf1 receptor Kremen1 has an intrinsic pro-apoptotic activity

We then investigated the possibility that Dkk1 negatively regulates a pro-apoptotic signaling triggered by one of its receptors. Such a mechanism implies that one (or more) of Dkk1 receptors behaves as a dependence receptor [1]. In order to assess whether Dkk1 receptors possess an intrinsic pro-apoptotic activity, we transfected HEK293T cells with plasmids encoding Krm1, Krm2 or Lrp6, and performed immunostaining against activated-Caspase-3 to reveal cells undergoing apoptosis [26]. As illustrated in Figure 2a-d, Krm1, but not Krm2 or Lrp6, expression resulted in a perinuclear accumulation of activated-Caspase-3.

In order to better understand how the apoptotic activity of Krm1 is regulated, we generated truncation mutants lacking either the extra- or intra-cellular domain. We found that deletion of the intracellular domain of Krm1 (ΔICD) completely abolished Caspase-3 activation (Figure 2e, f). On the contrary, a Krm1 construct devoid of extracellular domain (ΔECD), despite being expressed at lower levels, appeared hyperactive as it was able to elicit strong apoptotic signaling in almost all transfected cells (Figure 2g, h). These observations suggest that Krm1 apoptotic activity is mediated by its intracellular domain and negatively regulated by its extracellular domain, possibly through ligand binding.

Dickkopf1 inhibits the pro-apoptotic activity of Kremen1

Since Krm1 apoptotic activity appears regulated by extracellular signals, we tested the consequences of Dkk1 presence on this process. We found that co-transfection of Dkk1 was able to inhibit Krm1-induced Caspase-3 activation (Figure 3a-b). Quantifications indicated a ~40% to ~65% decrease (depending on the Dkk1/Krm1 ratio) in the proportion of active Caspase-3-positive cells among Krm1-transfected cells (Figure 3c), and the remaining

apoptotic cells displayed a 2- to 4-fold reduction in the levels of activated Caspase-3 fluorescence relative to HA fluorescence (Figure 3d).

We also assessed the ability of other known Krm1 ligands Dkk2, Dkk3, Dkk4 and R-spondin1 [17,27,28] to rescue Krm1-induced apoptosis. Although none of them were found as efficient as Dkk1, all were able to decrease Caspase-3 activation upon co-transfection with Krm1 in a significant and dose-dependent manner (Figure 3c).

We then tested whether Dkk1 can inhibit Krm1 apoptotic activity in a non-cell autonomous manner. We first applied soluble Dkk1 (using either a recombinant protein or a conditioned medium from Dkk1-transfected cells) on Krm1-transfected cells. In another set of experiments, we seeded Krm1-transfected cells on a carpet of Dkk1-expressing cells. In all cases we measured a significant decrease in the proportion of Caspase-3 positive cells among Krm1-transfected cells upon exposure to exogenous Dkk1 (Figure 3e-g). The fact that we never observed as good of a rescue using non-autonomous strategies as in co-transfection experiments could be due to protein stability/activity issues, as previously reported [29], or to the existence of a pool of Krm1 that would remain inaccessible (intracellular for example) to exogenous ligand. From these experiments, we concluded that Krm1 is a *bona fide* dependence receptor whose apoptotic activity is inhibited upon ligand binding in a dose dependent-manner.

Kremen1 and Dickkopf1 control cell survival in a Wnt-independent manner

Since Wnt-inhibition in cultured embryos is unable to mimic the anti-apoptotic effect of Dkk1, we decided to further investigate the relationship between Krm1-mediated Wnt-antagonism and apoptosis promotion.

Consistent with our whole embryo culture experiments, we found that treatment of Krm1-transfected cells with the Wnt inhibitor endo-IWR1 was unable to recapitulate the anti-

apoptotic effect of Dkk1 (Figure 4a). In addition, the Wnt-activator Azakenpaullone [30] proved unable to counterbalance Dkk1-mediated rescue of Krm1-induced apoptosis (Figure 4a). Together, these results indicate that the ability of Dkk1 to block apoptotic signaling downstream Krm1 is not mediated by Wnt-inhibition. We then performed Wnt-activity assays using the luciferase Wnt reporter TOPFlash. We found that HEK cells display an intrinsic Wnt activity that was significantly inhibited following Krm1 expression (Figure 4b). We observed a similar inhibition of Wnt signaling using the Krm1 ΔICD construct (Figure 4b) indicating that the intracellular domain of Krm1 is dispensable for Wnt antagonism, as previously shown for Krm2 [17]. Assessment of the consequence of Krm1 extracellular domain removal on Wnt inhibition proved more difficult to interpret as it appeared highly variable between experiments (Figure 4b). This is perhaps due to the strong apoptotic activity and low expression level of this construct (see Figure 2g). Thus, an apoptotically inactive mutant of Krm1 fully retains its ability to inhibit Wnt-signaling whereas an apoptotically hyperactive form only mediates weak (if any) Wnt-antagonism (Figure 4c). We therefore propose a model in which Krm1 display two independent signaling activities : Wnt inhibition through its extracellular domain in the presence of Dkk1 and apoptosis induction through its cytoplasmic domain in the absence of ligand (Figure 4d).

Kremen1 apoptotic activity is a recent evolutionary acquisition

Our data indicate that Krm2 does not share the same intrinsic apoptotic activity as Krm1, we therefore speculated that such an activity was acquired by Krm1 (or lost by Krm2) during evolution. In order to test our hypothesis and determine when the pro-apoptotic function might have arisen, we transfected cells with plasmids encoding chicken, xenopus and zebrafish Krm1. Incidentally, only one Krm1 ortholog was found in each of these species (compared sequences of the intracellular domains are shown in Figure 5a). Contrary to

mKrm1, we found cKrm1, xKrm1 and zKrm1 unable to induce Caspase-3 activation (Figure 5b-e, compare with Figure 2a). This may either result from a lack of intrinsic pro-apoptotic activity of chicken, xenopus and zebrafish Krm1 or from their inability to interact with the necessary partners in human cells. In order to distinguish between these two possibilities, we tested the ability of mKrm1 and cKrm1 to induce apoptosis in chick embryos using *in ovo* electroporation. As revealed by TUNEL staining, we found that mKrm1 is able to induce cell death in avian cells (Figure 5f, h), not only indicating that Krm1 is indeed apoptotic in an *in vivo* context, but also that the downstream signaling pathway most likely involves partners which are conserved between chick and mouse. Unlike its murine counterpart, cKrm1 was unable to trigger apoptosis *in ovo* (Figure 5g, h), further supporting the hypothesis of an evolutionary acquisition of a pro-apoptotic behavior by mKrm1.

We then aimed at identifying residues or motifs within the intracellular domain of mKrm1 that permit apoptotic signaling to occur. We first made the fortuitous observation that the addition of an epitope tag to the C-terminus of mKrm1 completely abolishes Caspase-3 activation (Figure 6a). We therefore speculated that the C-terminal domain of mKrm1 is essential for its pro-apoptotic function. Sequence comparison between mouse, chicken, xenopus and zebrafish Krm1 intracellular domains prompted us to focus on the last two residues of mKrm1, which are the only ones in the last dozen not to be found in any of the three other species (Figure 5a). We found that, in mKrm1, substitution of either one of the last two amino-acids by their chicken counterpart (S472G or D473N) completely abolished Caspase-3 activation (Figure 6a). Conversely, in cKrm1, substitution of the last two residues (GN) with their murine equivalent (SD) was sufficient to confer apoptotic activity, although not to a full extent, to the normally inactive chick protein (Figure 6b-e). We therefore concluded that C-terminal residues of mKrm1 are critical for triggering apoptosis.

Consistent with our previous observation that Wnt-antagonism is mediated by the extracellular domain, we found that the various mouse and chicken Krm1 constructs, that differ in their apoptotic activities, share the same ability to inhibit Wnt-signaling (Figure 6f), further confirming that Krm1-induced apoptosis is Wnt-independent.

Almost all Krm1 sequences of placental mammals we found in databases show strong conservation at the C-terminus (including SD residues), whereas none of the amphibians, sauropsids (birds, crocodiles and turtles) or bony fishes have the SD motif (Figure 6g). Moreover, among non-placental mammals, platypus has GY residues at the C-terminus, whereas the marsupials opossum and wallaby display a GD motif; sequences which are, according to our mutagenesis experiments, unlikely to allow apoptotic signaling in these three species. We therefore propose that the pro-apoptotic activity of Krm1 was acquired subsequent to the divergence between marsupials and placental mammals. Furthermore, in humans (as well as several primates) alternative splicing can yield an additional isoform that differs at the C-terminus, consisting in the replacement of the last 3 amino acids by a 20 amino acids-long tail (Figure 6g). We speculated that this "long" isoform would be apoptotically inactive and tested this hypothesis by substituting the last 3 amino acids of mKrm1 by the 20 amino acid tail. As illustrated Figure 6h, we found the long isoform unable to trigger apoptosis, further demonstrating the importance of the C-terminal sequence.

Kremen1 apoptotic activity is reduced by cancer mutations

Dependence receptors have been proposed to act as tumor suppressors and improper function of dependence receptors has been reported in cancers [1].

Consistent with an involvement of Krm1 in human cancers we found in TCGA (The cancer genome atlas; https://genome-cancer.ucsc.edu) [31] that various cancers fit within a pattern combining (i) high expression of Krm1 and low expression of Dkk1 in normal tissue, (ii)

decreased Krm1 expression in tumors, and/or (iii) increased Dkk1 expression in tumors (Supplementary Figure 3). To further question the contribution of Krm1-induced apoptosis in cancers, we interrogated the COSMIC database (catalogue of somatic mutations in cancer; http://www.sanger.ac.uk/cosmic) [32]. At the date we performed our studies (COSMIC v68 release, 4th February 2014), 45 unique samples bearing *krm1* mutations were reported (out of 8845), with some of these mutations being found in several independent samples. By contrast, only 12 mutations in *krm2* were found, all of them in unique samples and nearly half of them being coding silent. We decided to focus on the three missense point mutations identified within Krm1 intracellular domain: S421F (found in two colorectal and one ovary carcinoma samples), S439L (found in one lung carcinoma sample) and I455V (also found in one lung carcinoma sample). It is worth noting that a second sample (colorectal carcinoma) bearing the S439L mutation was added to the COSMIC database in a more recent release (v70 release, 14th August 2014).

In order to address whether these mutations affect Krm1 pro-apoptotic activity, we mutated the corresponding amino acids of mouse Krm1 (S419F, S437L and I453V) and proceeded with cell transfection (Figure 7a-d). We found that transfection with S419F or S437L mutants induced Caspase-3 activation in ~40% less cells than their wild-type counterpart (Figure 7e). In addition, we measured the intensity of activated Caspase-3 staining relative to HA staining per cell and found that all three mutations resulted in a significant reduction (Figure 7f). Importantly, and consistent with our previous finding, Krm1 cancer mutants appear equally able to antagonize Wnt-signaling as wild-type Krm1 (Figure 7g). We therefore concluded that Krm1 mutations found in human cancers can affect its apoptotic activity and propose that these mutations favor abnormal cancer cells survival and thus confer them a selective advantage (Figure 7h).

Discussion

We have unraveled an unexpected function for Dkk1 and Krm1 in regulating cell survival, in addition to (and independent of) their previously characterized role in Wnt-signaling. To our knowledge, it is the first demonstration of a Wnt-independent function for both Dkk1 and Krm1, and the first report of a biological function that is not shared by Krm1 and Krm2 as both were shown to equally mediate Dkk1-induced Wnt-inhibition [17].

A Krm2 truncation mutant lacking the entire intracellular domain was previously shown to retain its ability to mediate Wnt-inhibition [17]. Consistently, we found that Krm1 intracellular domain is also dispensable for Wnt-inhibition. Conversely, the cytoplasmic tail of Krm1 is strictly required for apoptotic signaling. Krm1 therefore appears as an atypical dependence receptor since its positive and negative signaling activities are regulated by topologically distinct domains.

In this study, we report for the first time a specific function for mouse Krm1 compared to its chick, xenopus and zebrafish orthologues. Interestingly, our cross-species electroporation experiments indicated that mKrm1 retains its apoptotic activity when expressed in avian cells. It is therefore reasonable to assume that the intracellular apoptotic signaling cascade was already present in the common ancestor to placental mammals. We can thus speculate that the acquisition of a pro-apoptotic behaviour by Krm1 occurred by a mechanism of molecular exaptation, consisting in the recruitment of a pre-existing functional pathway.

Loss of function experiments in xenopus demonstrated that Krm1 and Krm2 are required together for amphibian anterior nervous system development [24]. In mice however, *Krm1*$^{-/-}$; *Krm2*$^{-/-}$ animals are viable and display no obvious brain phenotype [33]. In these two species, requirement of Kremens during CNS development and apoptotic activity of Krm1 therefore appears inversely correlated. One possibility is that the acquisition of apoptotic behavior by Krm1 is simply not compatible with a strong requirement during development. Another

possibility is that the acquisition of apoptotic activity by Krm1 was accompanied by inhibitory mechanisms preventing deleterious functioning. Our expression data, consistent with other studies [18,19,24,34,35] indicate that *krm1* is a rather widely expressed gene during mouse embryonic development whereas *dkk1* expression is more spatially restricted. This may well reflect the existence of mechanisms negatively regulating Krm1-induced apoptosis, and whose identification will be one of the future challenges.

Cell death has not been investigated in the developing central nervous system of either *Krm1*$^{-/-}$ or *Dkk1*$^{-/-}$ embryos [19,33], although one can argue that in the case of Dkk1 mutants, the dramatic absence of induction of head structures does not allow such an analysis to be performed. Interestingly, in the hippocampus of adult mice, conditional tamoxifen-induced loss of Dkk1 was shown to results in an increase apoptosis that specifically affects DCX^{+} neuroblasts [36], supporting the hypothesis that Dkk1 can act as a survival factor in physiological conditions.

Most dependence receptors identified so far were involved in cancers, consistent with the idea that both receptor loss of function or ligand overexpression may confer a selective advantage to tumor cells by favoring their abnormal survival [1]. In the specific case of DCC, possibly the most studied dependence receptor, the tumor suppressor function has formally been demonstrated and attributed to its apoptotic activity [37]. *Dcc* mutations are found in ~2.5% of COSMIC samples compared to ~0.5% for *krm1*. However, since *dcc* is a gene three times longer than k*rm1*, and therefore more likely to accumulate mutations, the frequency of *krm1* mutations in cancers appears comparable to the one of *dcc*.

Identifying new dependence receptors remains of primary importance in the scope of providing alternative cancer therapies and diagnostic tools. New perspectives are currently arising, consisting in characterizing tumors which express both a dependence receptor and its ligand and trying to interfere with production of the latter [38-41]. We provide strong evidences supporting an evolutionary acquisition of dependence behavior for Krm1, which might be one

of the mechanisms by which placental mammals tackled the necessity to develop protective strategies against cancers. We further suggest that in humans, Krm1 apoptotic behavior can be regulated by alternative splicing. Prior to this study, Krm1 implication in cancers was rather lightly documented, only supported by the loss of expression observed in some cancer cell lines [35]. We now provide additional evidence by reporting that somatic mutations in cancer can affect Krm1 apoptotic activity without modifying its ability to inhibit Wnt-signaling. Although the cancer mutations we tested are not complete loss of apoptotic function, it is worth mentioning that such a possibility has been reported in at least two instances in the COSMIC database, corresponding to frameshift mutations at positions 251 and 438 that certainly abolish Krm1 apoptotic activity.

By contrast, the role of Dkk1 in cancers is already well established. Interestingly, despite the fact that all studies concur that Dkk1 acts through modulation of Wnt signaling, both positive and negative roles have been proposed [20-22]. Such a discrepancy could reflect Dkk1's dual function: as a Wnt antagonist Dkk1 would inhibit cancer progression, whereas the anti-apoptotic function we reveal would favor cancer cells survival. It is noteworthy that multiple studies provided proof of concept that Dkk1 targeting by immunotherapy can be used efficiently in both protective and therapeutic manners against cancer [42-47]. Sato and colleagues (2010) [46] found that anti-Dkk1 treatment was able to induce apoptosis of A549 lung cancer cells (which express high levels of Dkk1) by an unknown mechanism, which we believe could be the one we describe here. Furthermore, tumors formed in nude mice following A549 cells injection were significantly smaller in animals treated with anti-Dkk1 compared to controls, demonstrating that Dkk1 targeting by antibodies can efficiently inhibit tumor growth *in vivo* [46]. Our work will therefore not only shed a new light on Dkk1 and Krm1 function in development and cancer, but also (and more significantly) support efforts in developing therapies based on interfering with this novel pathway.

Materials and Methods

Animals

All animals used in this study were handled according to national regulations (approval #5096 from the French Ministry of Research on the use of genetically modified animals) and approved by the Veterinary Services of Paris (authorization to perform experiments on vertebrate animals #75-1454). Ablated embryos were obtained by mating *PGK:Cre* and *Dbx1*$^{LoxP\text{-}Stop\text{-}LoxP\text{-}DTA}$ animals as previously reported [23].

Constructs

The coding sequences of mouse *krm1*, *krm2*, *dkk1*, *dkk2*, *dkk3*, *dkk4* and *rspo1* were obtained following RNA extraction of E12.5 embryos using Trizol (Invitrogen), cDNA synthesis using SuperScript VILO (Invitrogen) and PCR amplification using Phusion polymerase (Thermo scientific). Human *lrp6* was amplified from I.M.A.G.E. clone #40125687. Chick, Xenopus and Zebrafish *krm1* were obtained from cDNA of HH14, stage 20 and 22 hpf embryos respectively. Constructs were made in pCAG-IRES-NLS-EGFP, mKrm1 was also cloned in pCS2. In some instances, an HA tag was inserted after the signal peptide. In the specific case of mKrm1 in pCS2, we found that adding the HA tag before the signal peptide had no incidence on expression levels, surface localization or apoptotic activity. For reasons that remain unclear, a better correlation between HA and Caspase-3 fluorescence intensities was observed with such a construct. Point mutations were generated using QuickChange site-directed mutagenesis kit (Stratagene), truncation or deletion mutants were produced by fusion PCR.

Culture

Whole embryo culture was performed in 75% rat serum (Charles River, Japan) in DMEM supplemented with penicillin and streptomycin using a 5% CO_2 incubator.

For immunofluorescence experiments, HEK293T cells were seeded on poly-L-lysine coated glass coverslips (in 15 mm wells) and cultured in 10% fetal bovine serum in DMEM supplemented with penicillin and streptomycin. Transfection was performed for 4 hours in Optimem using 2 µL Lipofectamine 2000 (Invitrogen) and 1 µg total DNA. Single transfections were achieved with 0.2 µg pCAG-construct + 0.8 µg empty pBluescript. Cotransfections were done using pCS2-Krm1 and pCAG-ligand in respective ratios of 0.5 µg / 0.5 µg (Figure 3a-d and 4a) or 0.2 µg / 0.8 µg (Figure 3c, d). Carpets of GFP^+ or $Dkk1^+$ cells were obtained by transfecting 1 µg pCAG-GFP or pCAG-Dkk1 ~4-6 h prior to seeding of dissociated $Krm1^+$ cells. Conditioned media were collected 24 h after transfection with 1 µg pCAG-GFP or pCAG-Dkk1.

For Wnt-activity assays, HEK293T cells were seeded on 96-well plates and transfected with 10 ng pRL-Renilla, 10 ng TOPFlash and 40 ng pCAG-Krm1 constructs (completed to 200 ng total DNA with empty pBluescript) using 0.4 µL Lipofectamine 2000 per well.

Recombinant mouse Dkk1 (R&D systems) was used at concentrations ranging from 0.1 to 1 µg/mL. We found the protein most efficient when used shortly after resuspension and therefore used only recently prepared aliquots. The Axin2 stabilizer Endo-IWR1 (Tocris) was used at concentrations ranging from 2 to 10 µM to inhibit Wnt signaling [25], the GSK-3β inhibitor 1-Azakenpaullone (Sigma-Aldrich) was used at concentrations ranging from 0.5 to 2 µM to activate Wnt signaling [30].

Staining

In situ hybridization and TUNEL were performed as previously described [23]. Immunostaining were performed 24 h after cell transfection, the following antibodies were used: mouse anti-

HA 16B12 (Convance, 1:1000), rabbit anti-cleaved Caspase-3 (Cell Signaling Technology, 1:1000), chick anti-GFP (Aves Labs, 1:2000). Secondary antibodies were coupled to Alexa488 (Invitrogen), Cy3 or Cy5 (Jackson Immunoresearch).

Wnt-activity assay

24 h after transfection, cells were rinsed in PBS and lysed in PLB buffer (Promega) for 25 min at room temperature. Firefly and Renilla luciferase activities were measured sequentially using the Dual Luciferase Reporter Assay kit (Promega) and a TriStar LB941 plate reader (Berthold Technologies).

Chick electroporation

Fertilized chick eggs were obtained from Morizeau (Dangers, France) and incubated at 37°C until HH10. Following DNA (4 µg/µL) injection in the spinal cord, 5 pulses of 25 V were applied using a CUY21 electroporator and CUY611P7-2 electrodes (Nepagene) to achieve unilateral transfection. Embryos were collected 24 h later.

Quantifications

Quantification of apoptosis in cultured embryos was achieved by counting the number of $TUNEL^+$ cells in the neural plate on 20 µm-thick section obtained from 3 to 5 embryos per condition. Means were compared using Student's t-test. Distributions were also compared by pooling all sections (n=25 to 36 depending on the condition) and applying the non-parametric Kolmogorov-Smirnov test. Quantification of apoptosis in HEK cells was achieved by counting the proportion of active $Caspase\text{-}3^+$ cells among GFP^+ (for untagged constructs) or HA^+ cells. Experiments were performed at least in triplicates. Approximately 200 GFP^+ or HA^+ cells were considered for each experiment. Histograms represent the means normalized

to 1 in control condition (usually Krm1 alone). Error bars on histograms correspond to standard deviations. Means were compared using Student's t-test. The activated Caspase-3 fluorescence relative to HA fluorescence was calculated for individual cells (the number of cells considered is indicated in the figure legends) and normalized to 1 in control condition. Distributions were compared using Kolmogorov-Smirnov test. Quantifications of Wnt-signaling activities in HEK cells was achieved by dividing the Firefly luciferase by Renilla in each well, and is expressed in relative luminescence units (RLU) normalized to 1 in control condition (untreated HEK cells). Experiments were performed at least in quadruplicates. Quantification of apoptosis in electroporated chick embryos was achieved by counting the number of $TUNEL^{+}$ cells per 100 µm of electroporated ventricular zone from a minimum of 6 sections belonging to at least three animals for each condition.

Acknowledgements

We are grateful to Thierry Galli, Anne Camus, Stéphane Nedelec, Eva Coppola and Sonia Garel for helpful discussions and critical reading of the manuscript. We wish to thank Anne Camus and Yoko Arai for their help in implementing whole embryo cultures, Christine Vesque and Sylvie Schneider-Maunoury for providing zebrafish cDNA, De-Li Shi for providing xenopus cDNA, Thierry Galli for providing HEK cells, Eve Gazave for her help regarding pharmacological agents, Anne-Laure Todeschini for her help with luciferase assays, Fabien Fauchereau for TCGA data mining, Lisa Vigier, Annie Dutriaux for technical assistance, Betty Freret-Hodara for helpful comments, Elenat Marot, Natalia Maties and Sébastien Gravat for maintaining mouse colonies, as well as the Imagoseine imaging facility. F.C. is an Inserm researcher. A.P. is a CNRS investigator and member Team of the Ecole des Neurosciences de Paris (ENP). This work was supported by grants from the Agence Nationale de la Recherche (ANR-2011-BSV4-023-01), the Fondation pour la Recherche Médicale (FRM) (INE20060306503), Ville de Paris (2006 ASES 102) and the Association pour la Recherche sur le Cancer (ARC) (SFI 2011 1203674) to A. P. and Comité de Paris de la Ligue contre le cancer (RS14/75-7 and RS15/75-46) to F. C.

Conflict of interest

The authors declare no conflict of interest.

References

1. Goldschneider D, Mehlen P. Dependence receptors: a new paradigm in cell signaling and cancer therapy. *Oncogene* 2010; **29:** 1865-1882.
2. Mehlen P, Rabizadeh S, Snipas SJ, Assa-Munt N, Salvesen GS, Bredesen DE. The DCC gene product induces apoptosis by a mechanism requiring receptor proteolysis. *Nature* 1998; **395:** 801-804.
3. Llambi F, Causeret F, Bloch-Gallego E, Mehlen P. Netrin-1 acts as a survival factor via its receptors UNC5H and DCC. *EMBO J* 2001; **20:** 2715-2722.
4. Thibert C, Teillet MA, Lapointe F, Mazelin L, Le Douarin NM, Mehlen P. Inhibition of neuroepithelial patched-induced apoptosis by sonic hedgehog. *Science* 2003; **301:** 843-846.
5. Tauszig-Delamasure S., Yu LY, Cabrera JR, Bouzas-Rodriguez J, Mermet-Bouvier C, Guix C *et al.* The TrkC receptor induces apoptosis when the dependence receptor notion meets the neurotrophin paradigm. *Proc Natl Acad Sci USA* 2007; **104:** 13361-13366.
6. Nikoletopoulou V, Lickert H, Frade JM, Rencurel C, Giallonardo P, Zhang L *et al.* Neurotrophin receptors TrkA and TrkC cause neuronal death whereas TrkB does not. *Nature* 2010; **467:** 59-63.
7. Luchino J, Hocine M, Amoureux MC, Gibert B, Bernet A, Royet A *et al.* Semaphorin 3E suppresses tumor cell death triggered by the plexin D1 dependence receptor in metastatic breast cancers. *Cancer Cell* 2013; **24:** 673-685.
8. Anastas JN, Moon RT. WNT signalling pathways as therapeutic targets in cancer. *Nat Rev Cancer* 2013; **13:** 11-26.
9. van Amerongen R, Nusse R. Towards an integrated view of Wnt signaling in development. *Development* 2009; **136:** 3205-3214.
10. Nusse R, Varmus HE. Many tumors induced by the mouse mammary tumor virus contain a provirus integrated in the same region of the host genome. *Cell* 1982; **31:** 99-109.
11. McMahon AP, Bradley A. The Wnt-1 (int-1) proto-oncogene is required for development of a large region of the mouse brain. *Cell* 1990; **62:** 1073-1085.
12. Angers S, Moon RT. Proximal events in Wnt signal transduction. *Nat Rev Mol Cell Biol* 2009; 10:468-477.
13. Cruciat CM, Niehrs C. Secreted and transmembrane wnt inhibitors and activators. *Cold Spring Harb Perspect Biol* 2013; **5:** a015081.
14. Bafico A, Liu G, Yaniv A, Gazit A, Aaronson SA. Novel mechanism of Wnt signalling inhibition mediated by Dickkopf-1 interaction with LRP6/Arrow. *Nat Cell Biol* 2001; **3:** 683-686.

15. Mao B, Wu W, Li Y, Hoppe D, Stannek P, Glinka A *et al.* LDL-receptor-related protein 6 is a receptor for Dickkopf proteins. *Nature* 2001; **411:** 321-325.

16. Semënov MV, Tamai K, Brott BK, Kühl M, Sokol S, He X. Head inducer Dickkopf-1 is a ligand for Wnt coreceptor LRP6. *Curr Biol* 2001; **11:** 951-961.

17. Mao B, Wu W, Davidson G, Marhold J, Li M, Mechler BM *et al.* Kremen proteins are Dickkopf receptors that regulate Wnt/beta-catenin signalling. *Nature* 2002; **417:** 664-667.

18. Glinka A, Wu W, Delius H, Monaghan AP, Blumenstock C, Niehrs C. Dickkopf-1 is a member of a new family of secreted proteins and functions in head induction. *Nature* 1998; **391:** 357-362.

19. Mukhopadhyay M, Shtrom S, Rodriguez-Esteban C, Chen L, Tsukui T, Gomer L *et al.* Dickkopf1 is required for embryonic head induction and limb morphogenesis in the mouse. *Dev Cell* 2001; **1:** 423-434.

20. Niehrs C. Function and biological roles of the Dickkopf family of Wnt modulators. *Oncogene* 2006; **25:** 7469-7481.

21. Rubin JS, Barshishat-Kupper M, Feroze-Merzoug F, Xi ZF. Secreted WNT antagonists as tumor suppressors: pro and con. *Front Biosci* 2006; **11:** 2093-2105.

22. Menezes ME, Devine DJ, Shevde LA, Samant RS. Dickkopf1: a tumor suppressor or metastasis promoter? *Int J Cancer* 2012; **130:** 1477-1483.

23. Causeret F, Ensini M, Teissier A, Kessaris N, Richardson WD, Lucas de Couville T *et al.* Dbx1-expressing cells are necessary for the survival of the mammalian anterior neural and craniofacial structures. *PLoS One* 2011; **6:** e19367.

24. Davidson G, Mao B, del Barco Barrantes I, Niehrs C. Kremen proteins interact with Dickkopf1 to regulate anteroposterior CNS patterning. *Development* 2002; **129:** 5587-5596.

25. Chen B, Dodge ME, Tang W, Lu J, Ma Z, Fan CW *et al.* Small molecule-mediated disruption of Wnt-dependent signaling in tissue regeneration and cancer. *Nat Chem Biol* 2009; **5:** 100-107.

26. Galluzzi L, Vitale I, Abrams JM, Alnemri ES, Baehrecke EH, Blagosklonny MV *et al.* Molecular definitions of cell death subroutines: recommendations of the Nomenclature Committee on Cell Death 2012. *Cell Death Differ* 2012; **19:** 107-120.

27. Binnerts ME, Kim KA, Bright JM, Patel SM, Tran K, Zhou M *et al.* R-Spondin1 regulates Wnt signaling by inhibiting internalization of LRP6. *Proc Natl Acad Sci USA* 2007; **104:** 14700-14705.

28. Nakamura RE, Hackam AS. Analysis of Dickkopf3 interactions with Wnt signaling receptors. *Growth Factors* 2010; **28:** 232-242.

29. De Langhe SP, Sala FG, Del Moral PM, Fairbanks TJ, Yamada KM, Warburton D *et al.* Dickkopf-1 (DKK1) reveals that fibronectin is a major target of Wnt signaling in branching morphogenesis of the mouse embryonic lung. *Dev Biol* 2005; **277:** 316-331.

30. Kunick C, Lauenroth K, Leost M, Meijer L, Lemcke T. 1-Azakenpaullone is a selective inhibitor of glycogen synthase kinase-3 beta. *Bioorg Med Chem Lett* 2004; **14:** 413-416.

31. Goldman M, Craft B, Swatloski T, Ellrott K, Cline M, Diekhans M *et al.* The UCSC Cancer Genomics Browser: update 2013. *Nucl Acids Res* 2012; **41:** D949-D954.

32. Forbes SA, Bindal N, Bamford S, Cole C, Kok CY, Beare D *et al.* COSMIC: mining complete cancer genomes in the Catalogue of Somatic Mutations in Cancer. *Nucleic Acids Res* 2011; **39:** D945-950.

33. Ellwanger K, Saito H, Clément-Lacroix P, Maltry N, Niedermeyer J, Lee WK *et al.* Targeted disruption of the Wnt regulator Kremen induces limb defects and high bone density. *Mol Cell Biol* 2008; **28:** 4875-4882.

34. Nakamura T, Aoki S, Kitajima K, Takahashi T, Matsumoto K, Nakamura T. Molecular cloning and characterization of Kremen, a novel kringle-containing transmembrane protein. *Biochim Biophys Acta* 2001; **1518:** 63-72.

35. Nakamura T, Nakamura T, Matsumoto K. The functions and possible significance of Kremen as the gatekeeper of Wnt signalling in development and pathology. *J Cell Mol Med* 2008; **12:** 391-408.

36. Seib DR, Corsini NS, Ellwanger K, Plaas C, Mateos A, Pitzer C *et al.* Loss of Dickkopf-1 restores neurogenesis in old age and counteracts cognitive decline. *Cell Stem Cell* 2013; **12:** 204-214

37. Castets M, Broutier L, Molin Y, Brevet M, Chazot G, Gadot N *et al.* DCC constrains tumour progression via its dependence receptor activity. *Nature* 2011; **482:** 534-537.

38. Fitamant J, Guenebeaud C, Coissieux MM, Guix C, Treilleux I, Scoazec JY *et al.* Netrin-1 expression confers a selective advantage for tumor cell survival in metastatic breast cancer. *Proc Natl Acad Sci USA* 2008; **105:** 4850-4855.

39. Delloye-Bourgeois C, Fitamant J, Paradisi A, Cappellen D, Douc-Rasy S, Raquin MA *et al.* Netrin-1 acts as a survival factor for aggressive neuroblastoma. *J Exp Med* 2009; **206:** 833-847.

40. Paradisi A, Maisse C, Coissieux MM, Gadot N, Lépinasse F, Delloye-Bourgeois C *et al.* Netrin-1 up-regulation in inflammatory bowel diseases is required for colorectal cancer progression. *Proc Natl Acad Sci USA* 2009; **106:** 17146-17151.

41. Paradisi A, Creveaux M, Gibert B, Devailly G, Redoulez E, Neves D *et al.* Combining chemotherapeutic agents and netrin-1 interference potentiates cancer cell death. *EMBO Mol Med* 2013; **5:** 1821-1834.

42. Fulciniti M, Tassone P, Hideshima T, Vallet S, Nanjappa P, Ettenberg SA *et al.* Anti-DKK1 mAb (BHQ880) as a potential therapeutic agent for multiple myeloma. *Blood* 2009; **114:** 371-379.

43. Glantschnig H, Hampton RA, Lu P, Zhao JZ, Vitelli S, Huang L *et al.* Generation and selection of novel fully human monoclonal antibodies that neutralize Dickkopf-1 (DKK1) inhibitory function in vitro and increase bone mass in vivo. *J Biol Chem* 2010; **285:** 40135-40147.

44. Pozzi S, Fulciniti M, Yan H, Vallet S, Eda H, Patel K *et al.* Scadden, H.M. Kronenberg, and N. Raje. In vivo and in vitro effects of a novel anti-Dkk1 neutralizing antibody in multiple myeloma. *Bone* 2013; **53:** 487-496.

45. Qian J, Zheng Y, Zheng C, Wang L, Qin H, Hong S *et al.* Active vaccination with Dickkopf-1 induces protective and therapeutic antitumor immunity in murine multiple myeloma. *Blood* 2012; **119:** 161-169.

46. Sato N, Yamabuki T, Takano A, Koinuma J, Aragaki M, Masuda K *et al.* Wnt inhibitor Dickkopf-1 as a target for passive cancer immunotherapy. *Cancer Res* 2010; **70:** 5326-5336.

47. Yaccoby S, Ling W, Zhan F, Walker R, Barlogie B, Shaughnessy Jr JD. Antibody-based inhibition of DKK1 suppresses tumor-induced bone resorption and multiple myeloma growth in vivo. *Blood* 2007; **109:** 2106-2111.

Titles and legends to figures

Figure 1. Dickkopf1 acts as a survival factor in a Wnt-independent manner. (**a**) Ablated *PGK:Cre;Dbx1*^{DTA} embryos cultured in the absence or presence of either recombinant Dkk1 or endo-IWR1 and stained by TUNEL. Top lane is a dorsal view (anterior is up, scale bar: 100 µm). Lower lane corresponds to cryostat sections (collected at the level of the dashed line) of the embryos shown above (scale bar: 100 µm). The neural plate is surrounded by a dashed line to allow a better visualization. (**b, c**) Histogram (mean ± sd) and cumulative distributions showing the number of TUNEL^{+} cells per section counted in ablated embryos untreated (35 sections from 5 animals), Dkk1-treated (25 sections from 3 animals at 0.2 µg/mL, 36 sections from 4 animals at 0.5 µg/mL and 34 sections from 4 animals at 1 µg/mL) or Endo-IWR1-treated (27 sections from 3 animals at 10 µM). * $p<0.01$ using Student's t-test and $p<0.003$ using Kolmogorov-Smirnov test, ** $p<0.003$ using Student's t-test and $p<0.001$ using Kolmogorov-Smirnov test, NS: non-significant.

Figure 2. Kremen1 has a pro-apoptotic activity. (**a-c**) HEK293T cells over-expressing Krm1 (**a**), Krm2 (**b**) or Lrp6 (**c**) are identified by nuclear GFP expression (green). Activated Caspase-3 is revealed by immunostaining (red). Scale bar: 10 µm. (**d**) Histogram representing the proportion of activated Caspase-3^{+} cells among GFP^{+} cells in the experiments shown in (**a-c**) and normalized to 1 (mean ± sd). * $p<0.001$ using Student's t-test. (**e-g**) HEK293T cells transfected with HA-tagged Krm1 full-length (**e**), lacking its intracellular domain (**f**) or lacking its extracellular domain (**g**). Cells were immunostained for HA (red) and activated Caspase-3 (green). Scale bar: 10 µm. (**h**) Quantification of the proportion of activated Caspase-3^{+} cells among HA^{+} cells normalized to 1 (mean ± sd) in the experiments shown in (**f-h**). * $p<0.001$ using Student's t-test.

Figure 3. Kremen1 is a dependence receptor for Dickkopf1. (**a, b**) HEK293T cells co-transfected with HA-tagged Krm1 (red) and either GFP (**a**) or Dkk1 (**b**) and immunostained for activated Caspase-3 (green). Scale bar: 10 µm. (**c**) Histogram of the proportion of activated Caspase-3^+ cells among Krm1-expressing cells upon co-transfection with increasing amounts of GFP or various Krm1 ligands and normalized to 1 (mean ± sd), * $p<0.001$ and § $p<0.01$ using Student's t-test. (**d**) Quantification of the activated Caspase-3 fluorescence relative to HA fluorescence per cell measured for n=139, 58, 120 and 63 Caspase-3^+ cells. Each dot represents one cell, log2 scale, *$p<0.001$ using Kolmogorov-Smirnov test. (**e**) Quantification of the proportion of activated Caspase-3^+ cells among Krm1-HA^+ cells normalized to 1 (mean ± sd) in the absence or presence of 0.1, 0.2, 0.5 and 1 µg/mL recombinant Dkk1. * $p<0.001$ using Student's t-test. (**f**) Quantification of the proportion of activated Caspase-3^+ cells among Krm1-HA^+ cells cultured in a medium previously conditioned by GFP- or Dkk1-transfected cells, normalized to 1 (mean ± sd). * $p<0.001$ using Student's t-test. (**g**) Quantification of the proportion of activated Caspase-3^+ cells among Krm1-HA^+ cells seeded on a carpet of GFP or Dkk1-transfected cells. § $p<0.01$ using Student's t-test.

Figure 4. Kremen1 acts in a Wnt independent manner. (**a**) Quantification of the proportion of activated Caspase-3^+ cells among HA^+ cells following co-transfection with either Krm1 and GFP (black bars) or Krm1 and Dkk1 (grey bars). Inhibition of the Wnt pathway using increasing doses of endo-IWR1 does not affect Krm1-induced apoptosis. Activation of the Wnt pathway with increasing doses of Azakenpaullone has no effect on Dkk1-mediated rescue of Krm1-induced apoptosis, NS: non-significant. (**b**) Luciferase assay indicating the relative activity of the Wnt signaling pathway in cells transfected with Krm1 or Krm1 truncations, compared with control cells. mean ± sd, * $p < 0.001$ using Student's t-test, § $p <$

0.05 compared with control or with Krm1 using Student's t-test (**c**) Summary of apoptotic and anti-Wnt activities of Krm1 and its truncation mutants as shown in Figures 2h and 4b. (**d**) A model summarizing our findings: Krm1 mediates Wnt-inhibition in the presence of Dkk1 and triggers apoptosis in its absence.

Figure 5. Kremen1 apoptotic activity is not common among vertebrates. (**a**) Protein sequence comparison of the intracellular domain of Krm1 in mouse (amino-acids 414 to 473), chick (393 to 450), xenopus (396 to 452) and zebrafish (410 to 465). Conservation of residues is indicated below according to the nomenclature of the ClustalX2 software. (**b-d**) HEK293T cells transfected with cKrm1 (**b**), xKrm1 (**c**), or zKrm1 (**d**) are identified by GFP expression (green). Activated Caspase-3 immunostaining (in red) is negative in all three conditions. Scale bar in (**b**): 10 µm. (**e**) Histogram representing the proportion of activated Caspase-3^+ cells among GFP^+ cells in the experiments shown in (**b-d**) and normalized to 1 (mean ± sd). * $p < 0.001$ using Student's t-test. (**f, g**) Cryosections of chick spinal cord electroporated with HA-tagged mKrm1 (**f**) or cKrm1 (**g**). Transfected cells are shown in red (HA immunolabelling) and apoptotic cells in green (TUNEL staining). Scale bar in (**f**): 20 µm. (**h**) Histogram representing the number of apoptotic cells counted per 100µm of electroporated ventricular zone in the experiments shown in (**f, g**) (mean ± sd). * $p < 0.001$ using Student's t-test.

Figure 6. Kremen1 C-terminal domain is responsible for apoptotic signalling. (**a**) Quantification of the proportion of activated Caspase-3^+ cells among HA^+ cells following transfection of mKrm1, Krm1 bearing a C-terminal Flag tag or point mutants S472G and D473N, normalised to 1 (mean ± sd). * $p<0.001$ using Student's t-test. (**b-d**) HEK293T cells transfected with HA-tagged mKrm1 (**b**), cKrm1 (**c**), or a modified cKrm1 bearing S and D residues at the C-terminus (**d**). HA^+ transfected cells are shown in red and activated Caspase-

3^+ cells in green. Scale bar in (**b**): 10 µm. (**e**) Quantification of the proportion of activated Caspase-3^+ cells among HA^+ cells in the experiments shown in (**b-d**) normalized to 1 (mean ± sd). * $p<0.001$ using Student's t-test. (**f**) Luciferase assay indicating the relative activity of the Wnt signaling pathway (mean ± sd) in cells transfected with wild-type or mutant mouse and chicken Krm1 constructs. * $p<0.001$ using Student's t-test. NS: non-significant. (**g**) Phylogenetic tree of various vertebrates for which a *krm1* sequence was found. Length of the branches is arbitrary. Species in bold are those for which we tested Krm1 apoptotic activity. RefSeq accession numbers are given when available. The two human sequences are generated by alternative splicing. * indicate cases where several sequences were found but with identical C-termini. # Sloth and armadillo sequences were manually reconstructed using Ensembl. § Opossum and platypus sequences are referenced in UniProtKB under the accession numbers H9H6Q3 and F7FX81 respectively. Protein sequences of the C-termini were aligned. Residues identical to the mouse sequence are highlighted in green. Residues that differ from the mouse sequence are indicated in red when located at positions that are critical for Krm1 apoptotic activity and in yellow otherwise. The red circle on the phylogenetic tree represents the stage at which the apoptotic activity of Krm1 was most likely acquired (lineage of the placental mammals). (**h**) Histogram representing the proportion of activated Caspase-3^+ cells among GFP^+ cells following transfection of mKrm1 or a modified version bearing the same C-terminus as the human long isoform, normalized to 1 (mean ± sd). * $p<0.001$ using Student's t-test.

Figure 7. Somatic mutations found in human cancers can affect Krm1 pro-apoptotic activity. (**a-d**) HEK293T cells expressing HA-tagged mKrm1 (**a**) or cancer mutants S419F (**b**) S437L (**c**) and I453V (**d**). Immunostaining revealed HA^+ cells in red and activated Caspase-3 in green. Scale bar in (**a**): 10 µm. (**e**) Quantifications the proportion of activated Caspase-3-

positive cells among HA-positive cells in the experiments shown in (**a-d**), normalized to 1 (mean ± sd), * p<0.001 using Student's t-test. NS: non-significant. (**f**) Quantification of the activated Caspase-3 fluorescence relative to HA fluorescence per cell measured for n=171 (Krm1), 107 (S419F), 110 (S437L) and 89 (I453V) cells. Each dot represent one cell, * p<0.001 using Kolmogorov-Smirnov test. (**g**) Luciferase assay indicating the relative activity of the Wnt signaling pathway in cells transfected with wild-type Krm1 or cancer mutants. * p<0.001 using Student's t-test. NS: non-significant. (**h**) Proposed model: Krm1 apoptotic activity favors the elimination of abnormal cells; mutations affecting its ability to activate Caspase-3 may confer a selective advantage to cancer cells.

Supplementary Figure 1. Dkk1 and its receptors are expressed in the developing brain. (**a**) We have previously shown that unknown secreted signals promote the survival of anterior neural plate cells in E8.25 mouse embryos. Hb: hindbrain, Mb: midbrain, Fb: forebrain. (**b, c**) *Dkk1* expression is detected at the midbrain/forebrain boundary at E8.25 (**b**) and in the forebrain at E8.5 (**c**). Scale bar in (**b**): 100 µm. (**d-f**) Expression of Dkk1 receptors *krm1* (**d**), *krm2* (**e**) and *lrp6* (**f**) is detected at high levels in the forebrain at E8.5; *lrp6* is additionally expressed in the dorsal midbrain and hindbrain (**f**). *In situ* hybridization experiments shown in (**d-f**) were deliberately under-developed and therefore indicate regions of highest expression.

Supplementary Figure 2. Whole embryo culture system. (**a**) Genetic ablation of $Dbx1^{+}$ cells is achieved by crossing *PGK:Cre* and $Dbx1^{LoxP\text{-}Stop\text{-}LoxP\text{-}DTA}$ animals. (**b**) Embryos were collected at E7.5 and cultured for 24 h. Scale bar in (**b**): 200 µm. (**c-d**) TUNEL staining of cultured embryos revealed few apoptotic cells in control embryos (**c**) whereas ablated *PGK:Cre* ; $Dbx1^{DTA}$ embryos (**d**) displayed a severe increase in apoptosis in the midbrain and forebrain (arrowheads). Scale bar in (**c**): 100 µm.

Supplementary Figure 3. *Krm1* and *Dkk1* expression in various cancers. (**a**) TCGA-extracted *krm1* expression level measured by RNAseq in tumors (red) and matching normal tissue (green) from the same patient (each bar represent one individual). n=113 for breast cancer, 31 for colorectal cancer, 41 for head and neck cancer, 72 for kidney clear cell cancer, 32 for kidney papillary cell cancer and 59 for thyroid cancer. *Krm1* expression is decreased in most tumors compared to normal tissue. (**b**) TCGA-extracted *dkk1* expression level measured by RNAseq in tumors (orange) and matching normal tissue (blue) from the same patient (each bar represent one individual). *Dkk1* expression is low in control tissue and upregulated in many tumors. (**c**) Ratio between *Krm1* expression in tumors and normal tissue for each patient (one bar represent one individual). In a majority of cases (the exact value is indicated for each type of cancer), the ratio falls below 1, corresponding to a decrease of *krm1* expression in the tumor sample compared to matching normal tissue from the same patient.

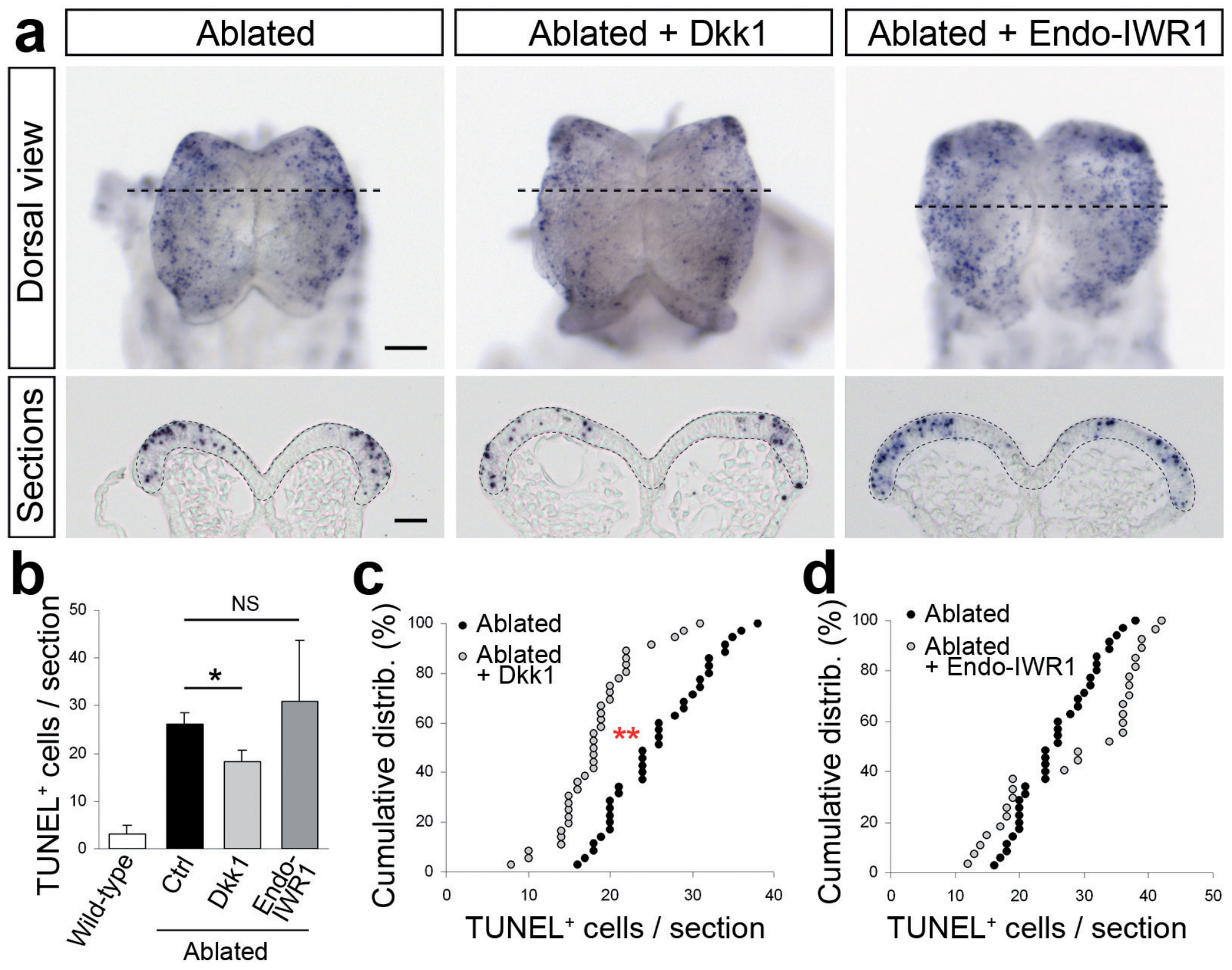
a
Ablated
Ablated + Dkk1
Ablated + Endo-IWR1
Dorsal view
Sections
b
TUNEL⁺ cells / section
NS
*
Wild-type
Ctrl
Dkk1
Endo-IWR1
Ablated
c
Cumulative distrib. (%)
Ablated
Ablated + Dkk1
**
TUNEL⁺ cells / section
d
Cumulative distrib. (%)
Ablated
Ablated + Endo-IWR1
TUNEL⁺ cells / section

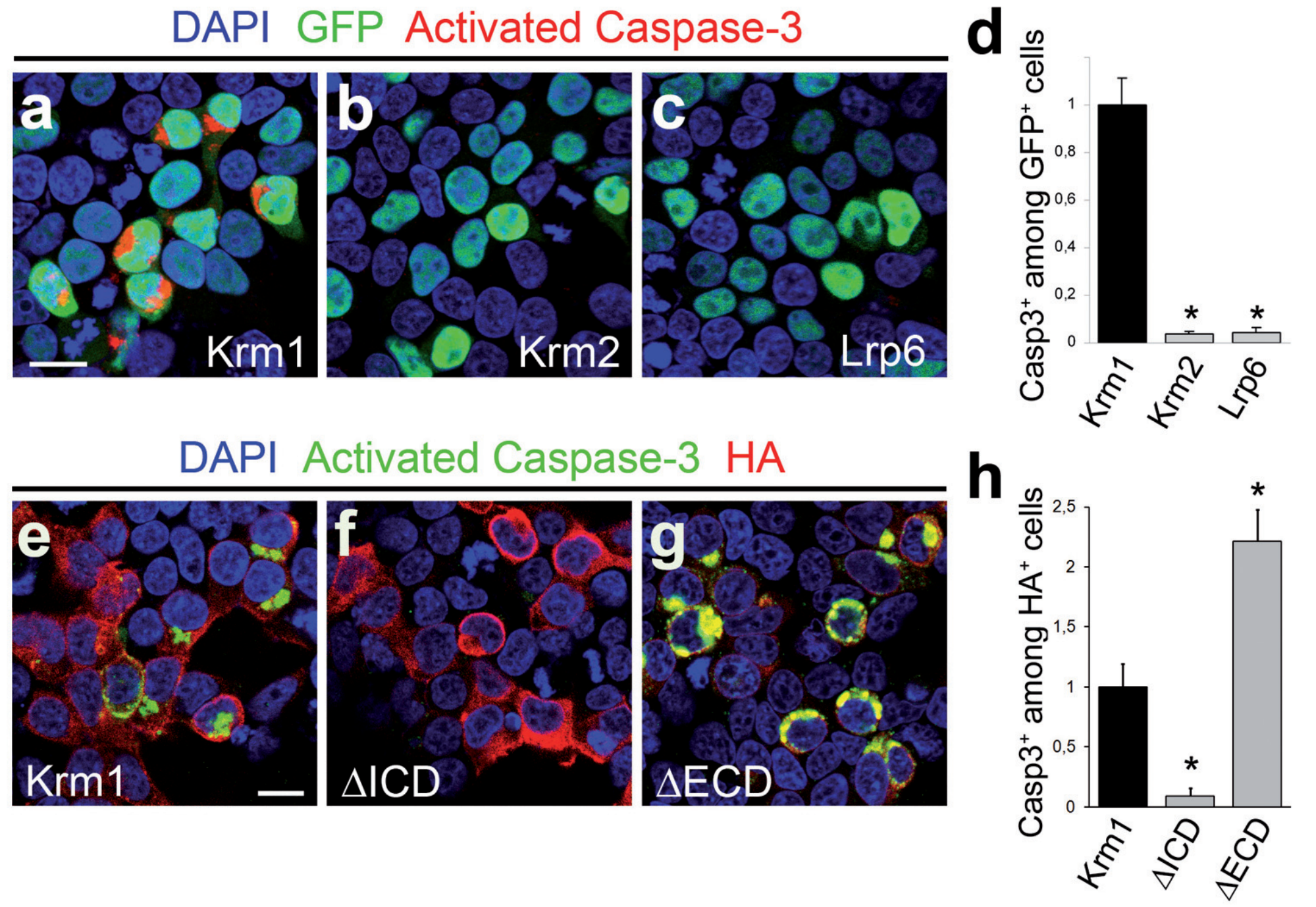
DAPI GFP Activated Caspase-3
a
Krm1
b
Krm2
c
Lrp6
d
Casp3+ among GFP+ cells
1
0,8
0,6
0,4
0,2
0
*
*
Krm1
Krm2
Lrp6
DAPI Activated Caspase-3 HA
e
Krm1
f
ΔICD
g
ΔECD
h
Casp3+ among HA+ cells
2,5
2
1,5
1
0,5
0
*
*
Krm1
ΔICD
ΔECD

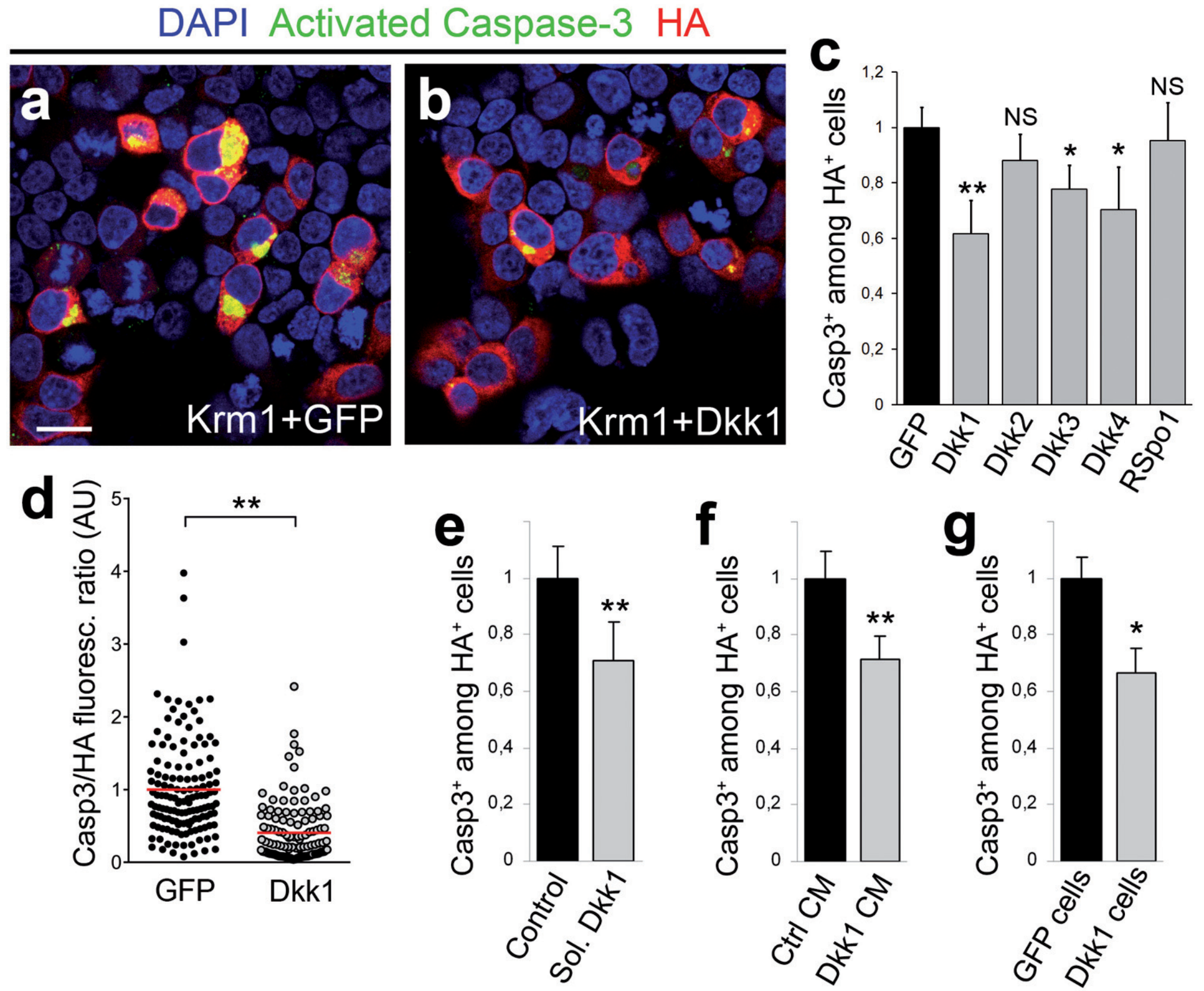
DAPI Activated Caspase-3 HA
a
Krm1+GFP
b
Krm1+Dkk1
c
Casp3+ among HA+ cells
1,2
1
0,8
0,6
0,4
0,2
0
**
NS
*
*
NS
GFP
Dkk1
Dkk2
Dkk3
Dkk4
RSpo1
d
Casp3/HA fluoresc. ratio (AU)
5
4
3
2
1
0
**
GFP
Dkk1
e
Casp3+ among HA+ cells
1
0,8
0,6
0,4
0,2
0
**
Control
Sol. Dkk1
f
Casp3+ among HA+ cells
1
0,8
0,6
0,4
0,2
0
**
Ctrl CM
Dkk1 CM
g
Casp3+ among HA+ cells
1
0,8
0,6
0,4
0,2
0
*
GFP cells
Dkk1 cells

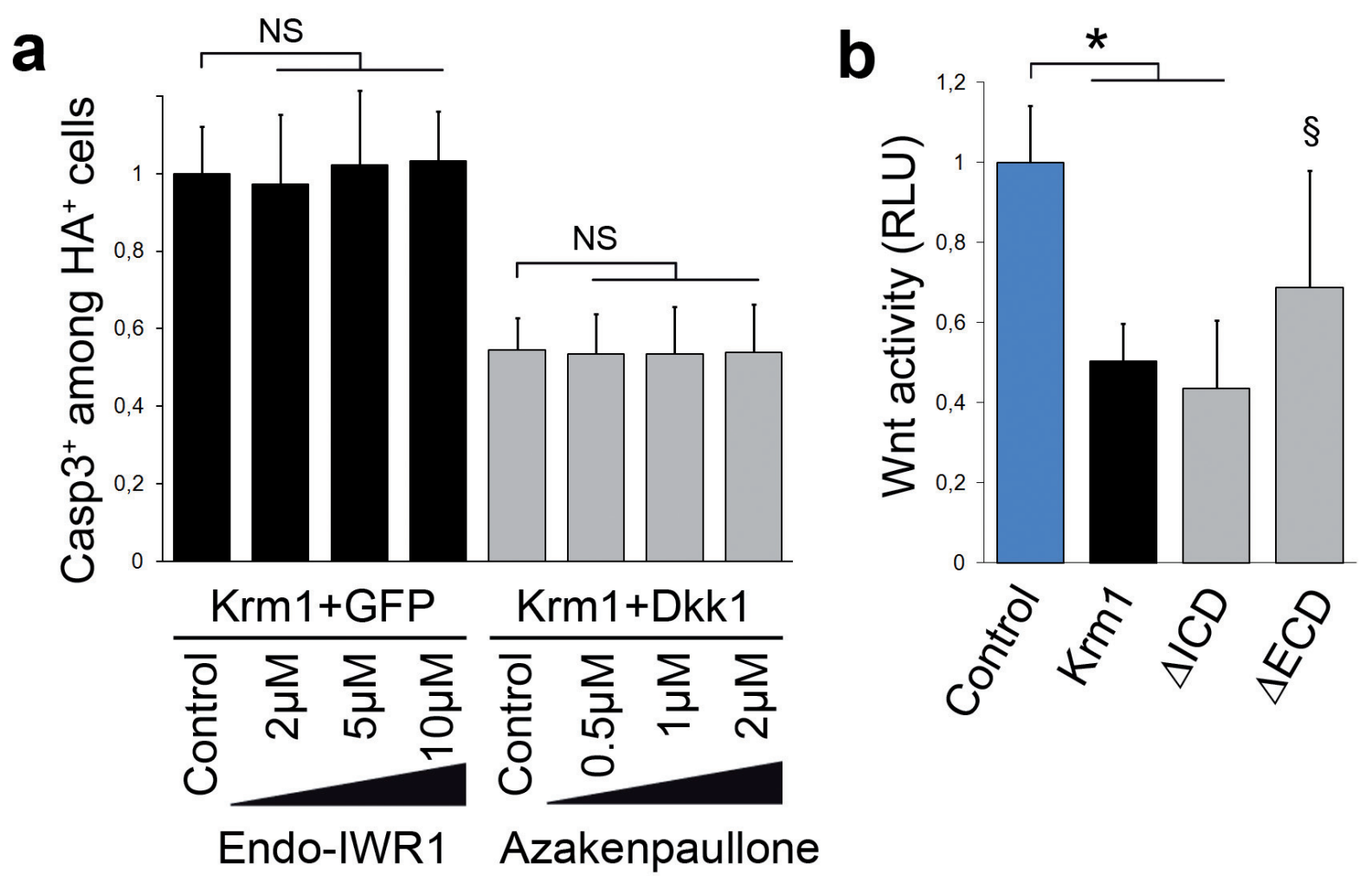

c

	Apoptotic activity	Wnt inhibition
Krm1	+	+
ΔICD	-	+
ΔECD	++	+/- (?)

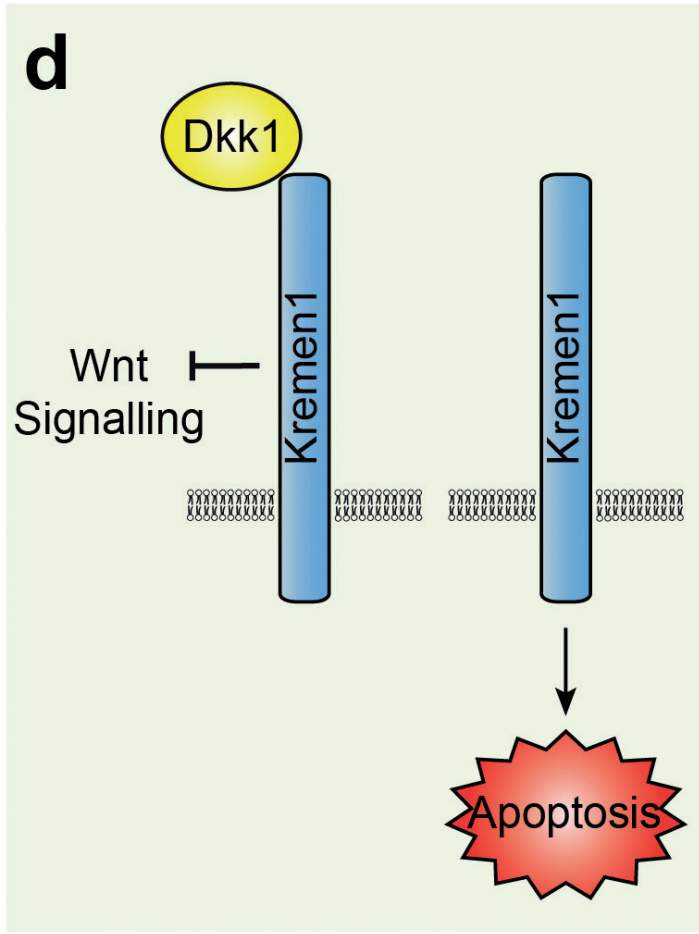

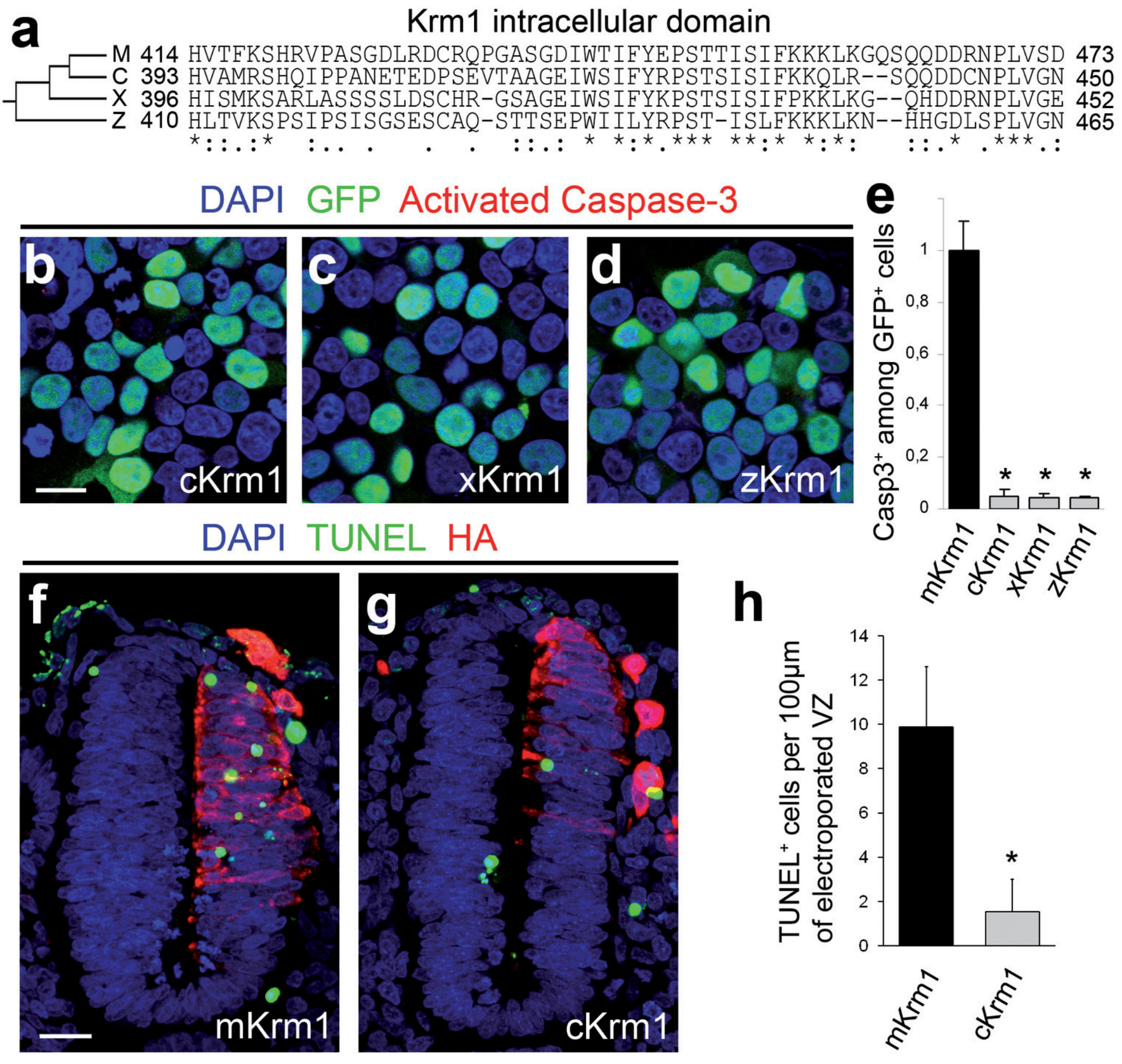
a
Krm1 intracellular domain
M 414 HVTFKSHRVPASGDLRDCRQPGASGDIWTIFYEPSTTISIFKKKLKGQSQQDDRNPLVSD 473
C 393 HVAMRSHQIPPANETEDPSEVTAAGEIWSIFYRPSTSISIFKKQLR--SQQDDCNPLVGN 450
X 396 HISMKSARLASSSSLDSCHR-GSAGEIWSIFYKPSTSISIFPKKLKG--QHDDRNPLVGE 452
Z 410 HLTVKSPSIPSISGSESCAQ-STTSEPWIILYRPST-ISLFKKKLKN--HHGDLSPLVGN 465
DAPI GFP Activated Caspase-3
b
cKrm1
c
xKrm1
d
zKrm1
e
Casp3+ among GFP+ cells
1
0,8
0,6
0,4
0,2
0
*
*
*
mKrm1
cKrm1
xKrm1
zKrm1
DAPI TUNEL HA
f
mKrm1
g
cKrm1
h
TUNEL+ cells per 100µm of electroporated VZ
14
12
10
8
6
4
2
0
*
mKrm1
cKrm1

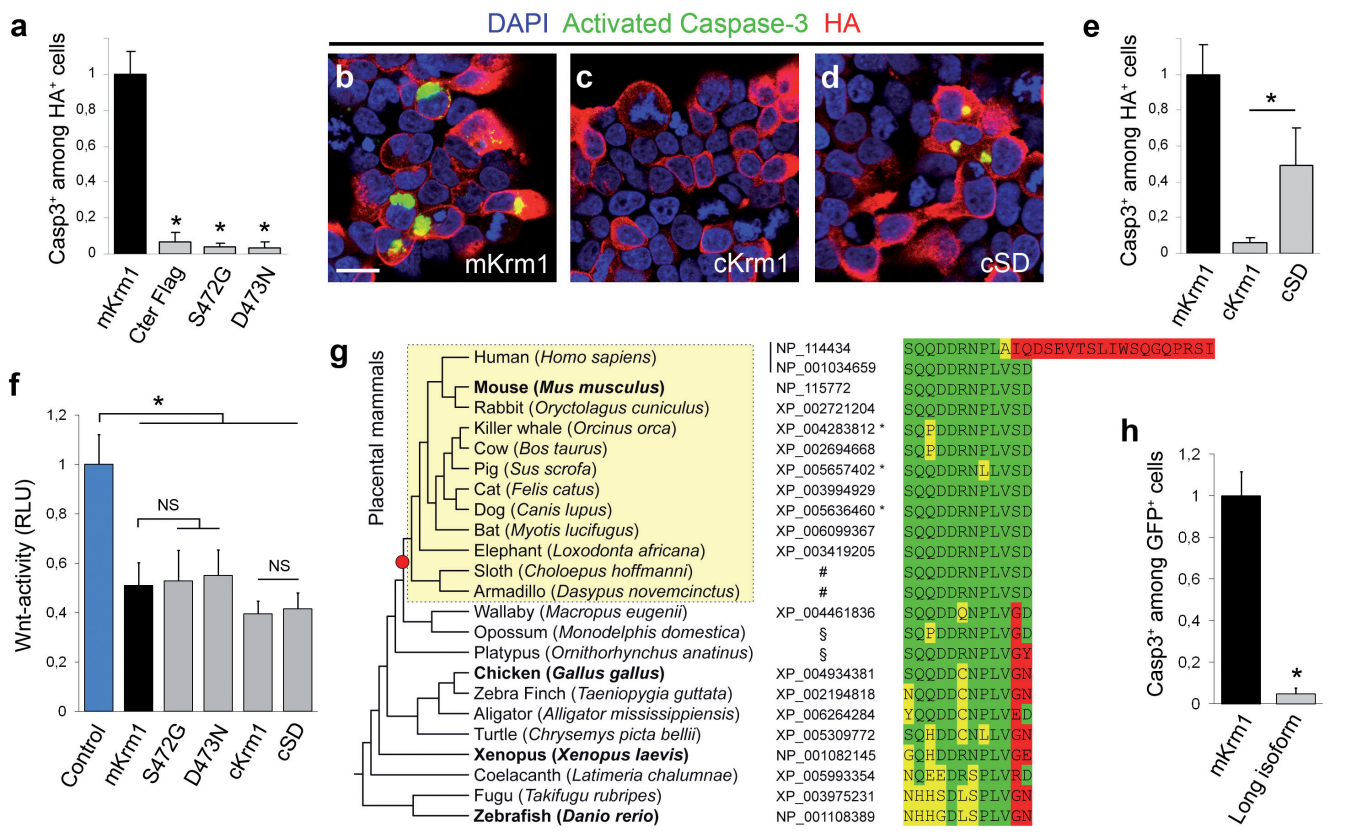
a
Casp3+ among HA+ cells
1
0,8
0,6
0,4
0,2
0
*
*
*
mKrm1
Cter Flag
S472G
D473N
DAPI Activated Caspase-3 HA
b
mKrm1
c
cKrm1
d
cSD
e
Casp3+ among HA+ cells
1
0,8
0,6
0,4
0,2
0
*
mKrm1
cKrm1
cSD
f
Wnt-activity (RLU)
1,2
1
0,8
0,6
0,4
0,2
0
*
NS
NS
Control
mKrm1
S472G
D473N
cKrm1
cSD
g
Placental mammals
Human (Homo sapiens)
Mouse (Mus musculus)
Rabbit (Oryctolagus cuniculus)
Killer whale (Orcinus orca)
Cow (Bos taurus)
Pig (Sus scrofa)
Cat (Felis catus)
Dog (Canis lupus)
Bat (Myotis lucifugus)
Elephant (Loxodonta africana)
Sloth (Choloepus hoffmanni)
Armadillo (Dasypus novemcinctus)
Wallaby (Macropus eugenii)
Opossum (Monodelphis domestica)
Platypus (Ornithorhynchus anatinus)
Chicken (Gallus gallus)
Zebra Finch (Taeniopygia guttata)
Aligator (Alligator mississippiensis)
Turtle (Chrysemys picta bellii)
Xenopus (Xenopus laevis)
Coelacanth (Latimeria chalumnae)
Fugu (Takifugu rubripes)
Zebrafish (Danio rerio)
NP_114434 SQQDDRNPLAIQDSEVTSLIWSQGQPRSI
NP_001034659 SQQDDRNPLVSD
NP_115772 SQQDDRNPLVSD
XP_002721204 SQQDDRNPLVSD
XP_004283812 * SQPDDRNPLVSD
XP_002694668 SQPDDRNPLVSD
XP_005657402 * SQQDDRNLLVSD
XP_003994929 SQQDDRNPLVSD
XP_005636460 * SQQDDRNPLVSD
XP_006099367 SQQDDRNPLVSD
XP_003419205 SQQDDRNPLVSD
SQQDDRNPLVSD
SQQDDRNPLVSD
XP_004461836 SQQDDQNPLVGD
§ SQPDDRNPLVGD
§ SQQDDRNPLVGY
XP_004934381 SQQDDCNPLVGN
XP_002194818 NQQDDCNPLVGN
XP_006264284 YQQDDCNPLVED
XP_005309772 SQHDDCNLLVGN
NP_001082145 GQHDDRNPLVGE
XP_005993354 NQEEDRSPLVRD
XP_003975231 NHHSDLSPLVGN
NP_001108389 NHHGDLSPLVGN
h
Casp3+ among GFP+ cells
1,2
1
0,8
0,6
0,4
0,2
0
*
mKrm1
Long isoform

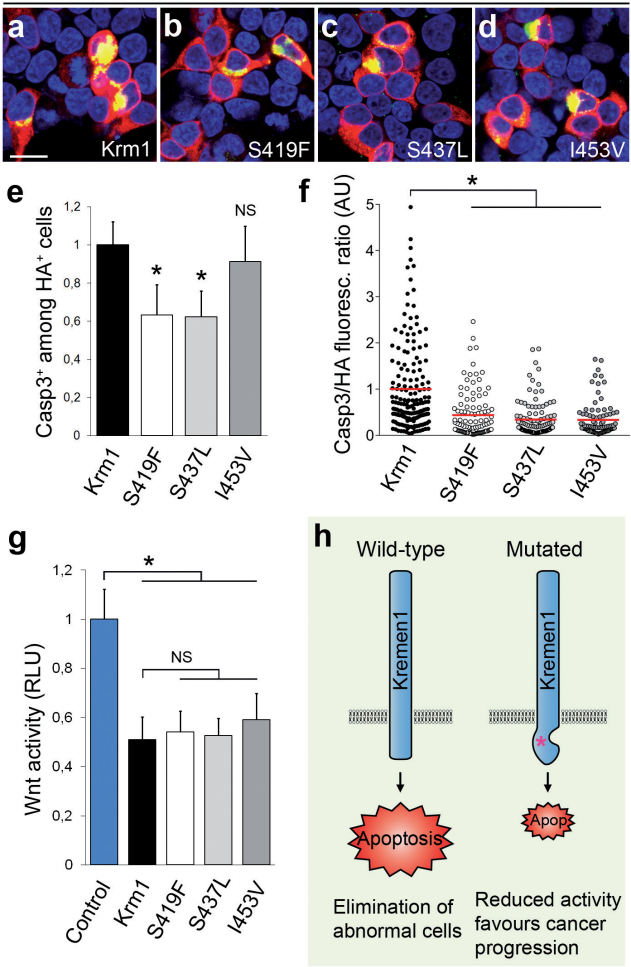
DAPI Activated Caspase-3 HA
a
b
c
d
Krm1
S419F
S437L
I453V
e
Casp3+ among HA+ cells
1,2
1
0,8
0,6
0,4
0,2
0
NS
*
*
Krm1
S419F
S437L
I453V
f
Casp3/HA fluoresc. ratio (AU)
5
4
3
2
1
0
*
Krm1
S419F
S437L
I453V
g
Wnt activity (RLU)
1,2
1
0,8
0,6
0,4
0,2
0
*
NS
Control
Krm1
S419F
S437L
I453V
h
Wild-type
Mutated
Kremen1
Kremen1
Apoptosis
Apop
Elimination of abnormal cells
Reduced activity favours cancer progression

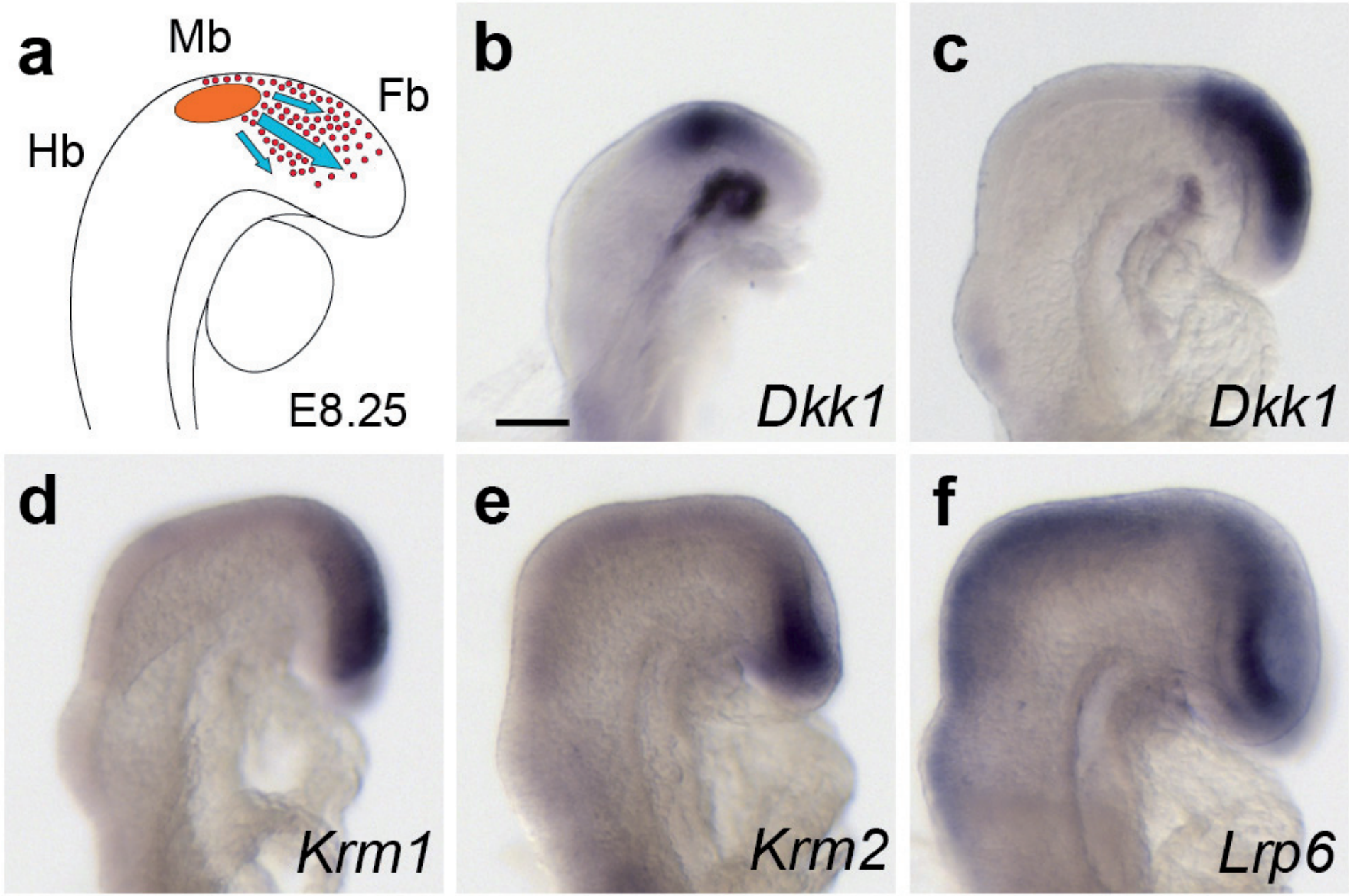
a
Mb
Fb
Hb
E8.25
b
Dkk1
c
Dkk1
d
Krm1
e
Krm2
f
Lrp6

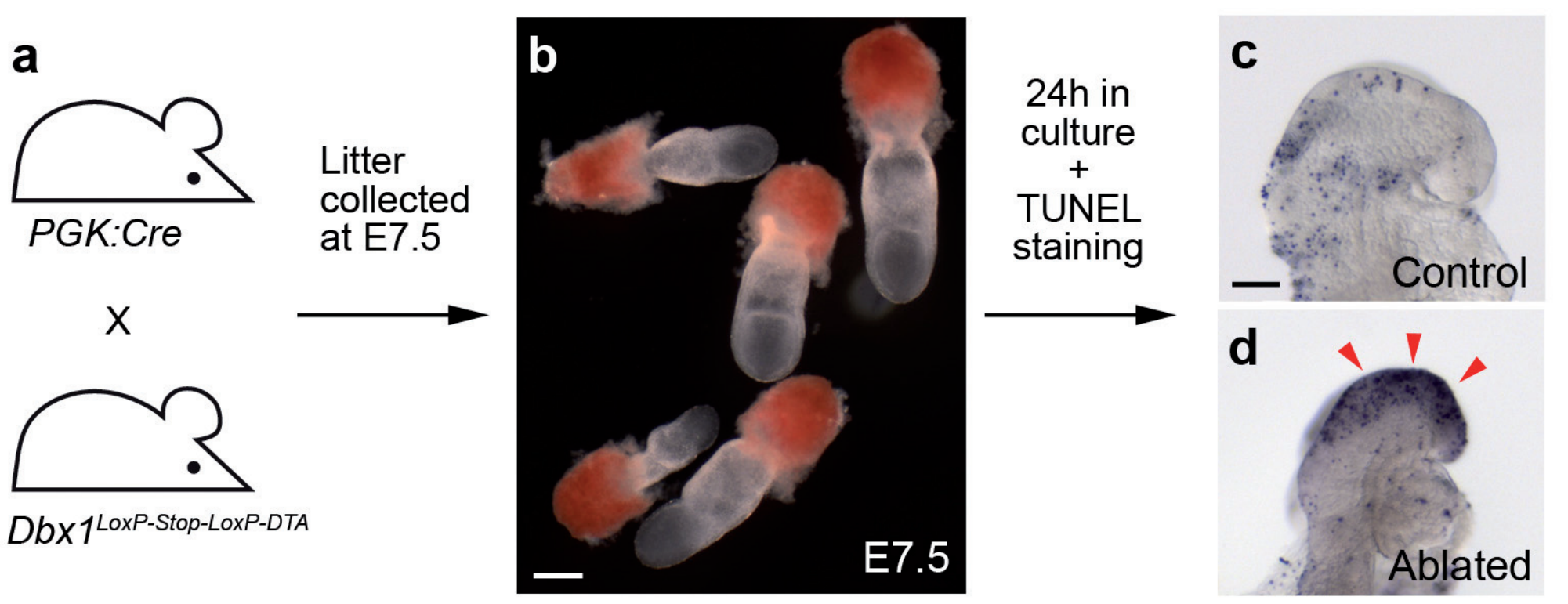
a
PGK:Cre
X
Dbx1LoxP-Stop-LoxP-DTA
Litter collected at E7.5
b
E7.5
24h in culture + TUNEL staining
c
Control
d
Ablated

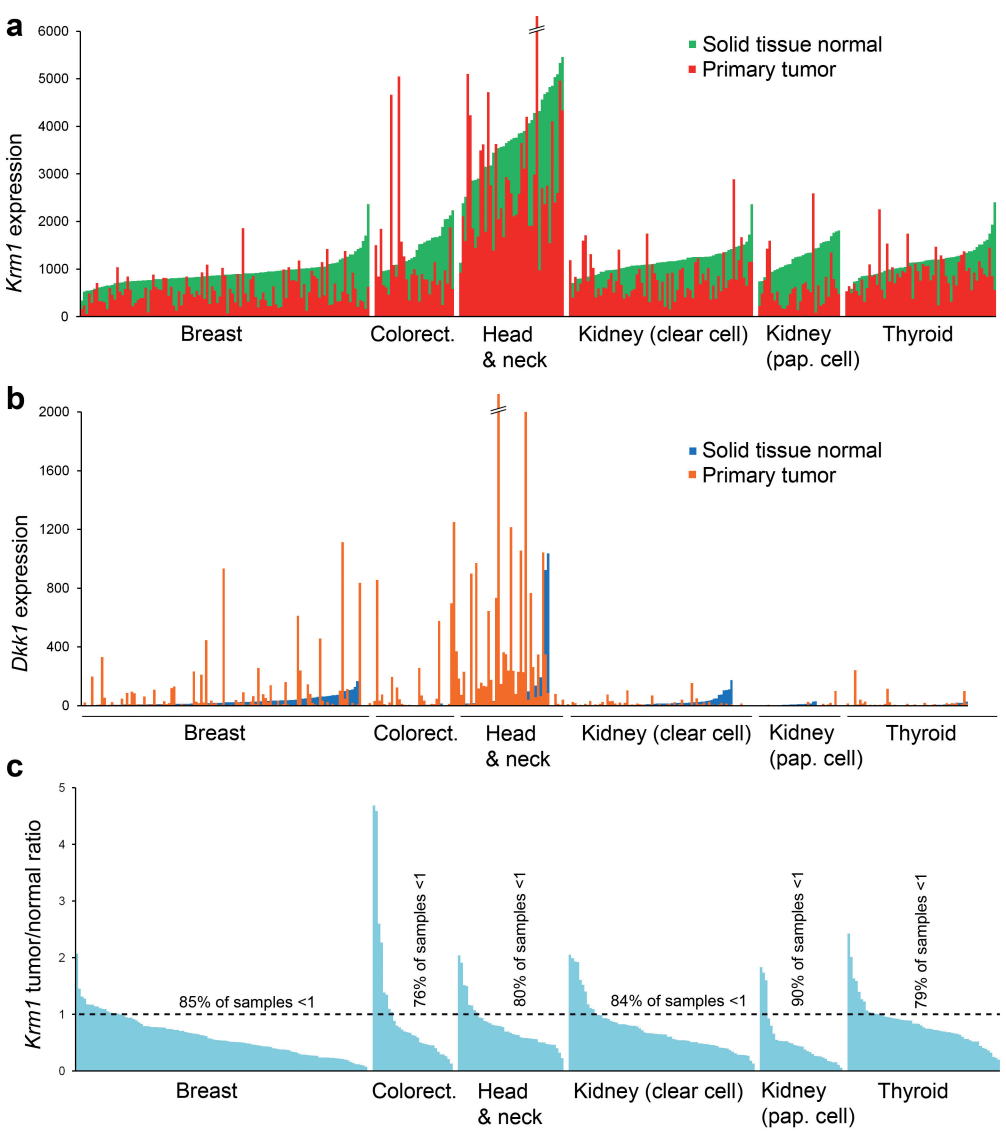
a
Krm1 expression
6000
5000
4000
3000
2000
1000
0
Solid tissue normal
Primary tumor
Breast
Colorect.
Head & neck
Kidney (clear cell)
Kidney (pap. cell)
Thyroid
b
Dkk1 expression
2000
1600
1200
800
400
0
Solid tissue normal
Primary tumor
Breast
Colorect.
Head & neck
Kidney (clear cell)
Kidney (pap. cell)
Thyroid
c
Krm1 tumor/normal ratio
5
4
3
2
1
0
85% of samples <1
76% of samples <1
80% of samples <1
84% of samples <1
90% of samples <1
79% of samples <1
Breast
Colorect.
Head & neck
Kidney (clear cell)
Kidney (pap. cell)
Thyroid